



# 14-3-3 $\gamma$ Haploinsufficient Mice Display Hyperactive and Stress-sensitive Behaviors

Do Eon Kim<sup>1†</sup>, Chang-Hoon Cho<sup>2†</sup>, Kyoung Mi Sim<sup>2</sup>, Osung Kwon<sup>2</sup>,  
Eun Mi Hwang<sup>3</sup>, Hyung-Wook Kim<sup>1\*</sup> and Jae-Yong Park<sup>2\*</sup>

<sup>1</sup>College of Life Sciences, Sejong University, Seoul 05006, <sup>2</sup>School of Biosystem and Biomedical Science, College of Health Science, Korea University, Seoul 02708, <sup>3</sup>Center for Functional Connectomics, Korea Institute of Science and Technology (KIST), Seoul 02792, Korea

14-3-3 $\gamma$  plays diverse roles in different aspects of cellular processes. Especially in the brain where 14-3-3 $\gamma$  is enriched, it has been reported to be involved in neurological and psychiatric diseases (e.g. Williams-Beuren syndrome and Creutzfeldt-Jakob disease). However, behavioral abnormalities related to 14-3-3 $\gamma$  deficiency are largely unknown. Here, by using 14-3-3 $\gamma$  deficient mice, we found that homozygous knockout mice were prenatally lethal, and heterozygous mice showed developmental delay relative to wild-type littermate mice. In addition, in behavioral analyses, we found that 14-3-3 $\gamma$  heterozygote mice display hyperactive and depressive-like behavior along with more sensitive responses to acute stress than littermate control mice. These results suggest that 14-3-3 $\gamma$  levels may be involved in the developmental manifestation of related neuropsychiatric diseases. In addition, 14-3-3 $\gamma$  heterozygote mice may be a potential model to study the molecular pathophysiology of neuropsychiatric symptoms.

**Key words:** 14-3-3 $\gamma$ , Ywhag, Hyperactivity, Anxiety, Acute stress, ADHD

## INTRODUCTION

14-3-3 proteins are a family of ubiquitously expressed adaptor proteins that are involved in diverse cellular processes, such as intracellular signaling, cell-cycle control, apoptosis, neuronal migration, and protein trafficking by regulating hundreds of different “client” proteins [1-3]. 14-3-3 proteins act as a dimer by binding to phosphorylated target proteins at specific site(s), causing a con-

formational change [4]. The interaction of 14-3-3 proteins with specific partners affects their stability, localization, and activities within the cell [2-4].

Since 14-3-3 proteins are enriched in the brain, they have been reported to be involved in a broad range of brain functions, and neurological and psychiatric diseases [2, 5]. 14-3-3 proteins have also been shown to be involved in axon growth and pathfinding as well as neuronal regeneration [6, 7]. In addition, transgenic mice expressing difopein, a 14-3-3 peptide inhibitor, displayed impairments of hippocampus-dependent learning and memory tasks, and long-term synaptic plasticity of hippocampal synapses [8]. These mice also display schizophrenia-like behaviors [9].

The behavioral phenotypes of two 14-3-3 isoform-specific null mice have been reported [10, 11]. In these studies, 14-3-3 $\epsilon$  knockout (KO) mice displayed enhanced anxiety-like behaviors and memory deficits as well as morphological abnormalities in the

Received December 9, 2018, Revised January 16, 2019,  
Accepted January 18, 2019

\*To whom correspondence should be addressed.  
Jae-Yong Park, TEL: 82-2-3290-5637, FAX: 82-2-917-2388  
e-mail: jaeyong68@korea.ac.kr  
Hyung-Wook Kim, TEL: 82-2-3408-3202, FAX: 82-2-3408-4334  
e-mail: kimhyung@sejong.ac.kr

<sup>†</sup>These authors contribute equally for this study.

hippocampus [11]. 14-3-3 $\zeta$  KO mice displayed hyperactive behaviors and cognitive deficits, as well as abnormal neuronal migration in the hippocampus during development [10].

14-3-3 $\gamma$ , encoded by *ywhag* gene, is one of seven isoforms ( $\beta$ ,  $\gamma$ ,  $\epsilon$ ,  $\sigma$ ,  $\zeta$ ,  $\tau$ , and  $\eta$ ) and its increased expression has been reported in Creutzfeldt-Jakob disease and ischemia [12-14]. In addition, by directly interacting with ataxin-1 (spinocerebellar ataxia type 1),  $\alpha$ -synuclein (Parkinson's disease), and TSC2 (tuberous sclerosis complex 2), 14-3-3 $\gamma$  is deeply involved in these neuropsychiatric diseases [15-17]. In particular, examining the behavioral phenotypes of 14-3-3 $\gamma$  null mice is clinically important because 1) genetic mutations of *ywhag* gene have been recently associated in neurodevelopmental disorders and 2) the *ywhag* gene is located at 7q11.23; chromosomal abnormalities (deletion or duplication) at this locus are strongly linked to Williams-Beuren syndrome (WBS), which is presented with developmental delay, intellectual disabilities, and epilepsy [18-21].

14-3-3 $\gamma$  is broadly expressed in various tissues including brain, liver, heart, ovary, thymus, spleen, and placenta, and it is considered mainly as a cytosolic protein to interact with diverse "client" proteins [1, 22]. According to the Allen brain atlas database (<http://mouse.brain-map.org>), 14-3-3 $\gamma$  is broadly expressed throughout the whole brain including cerebral cortex and hippocampus as previously shown [23, 24]. Although 14-3-3 $\gamma$  has been previously shown to be expressed in neurons and astrocytes in the brain, cell-type specific expression pattern of 14-3-3 $\gamma$  is largely unknown [13, 24, 25].

Previously, we have shown that 14-3-3 $\gamma$  regulates neuronal differentiation and surface expression of TRPM4b, ANO1 and BEST1 [26-28]. In addition, previous studies also showed that both overexpression and shRNA-mediated silencing of 14-3-3 $\gamma$  in the embryonic mouse brain resulted in neuronal migration delay and morphological defects in the developing cerebral cortex [23, 24]. Thus, the expression of 14-3-3 $\gamma$  in the brain may be critical for proper brain function. Although a previous report showed that there was no apparent phenotype in 14-3-3 $\gamma$  null mice [29], here, we examined a new 14-3-3 $\gamma$  null mouse generated using a gene-trap strategy [30].

## MATERIALS AND METHODS

### Animals

Transgenic *ywhag* mouse (CARD ID 1461) were generated by a group at Kumamoto University. In brief, exchangeable gene trap pU-21W vector was used for random gene trap mutagenesis. pU-21W is a promoter trap vector with three stop codons which were arranged in upstream of the ATG of the  $\beta$ -galactosidase ( $\beta$ -geo)

in all three frames [30]. The strain name is depicted as B6;CB-YwhagGt (pU-21W)266Card, and the website address of the Database for the Exchange of Gene Trap Clones is [http://egtc.jp/action/access/clone\\_detail?id=21-W266](http://egtc.jp/action/access/clone_detail?id=21-W266). Littermates including *ywhag* wild-type (WT), heterozygote knockout (Het), and homozygote knockout (KO) mice were used for this study. Mice were housed and maintained in standard laboratory conditions of 12:12 h light:dark cycle. Regular chow and water were provided *ad libitum*. All animal experiments were performed in accordance with the guidelines of Sejong University and Korea University Institutional Animal Care and Use Committee. Male mice were used for behavioral experiments.

### Genotyping

*ywhag* KO (-/+ and -/-) mice were genotyped using polymerase chain reaction (PCR), and littermate *ywhag* (+/+) mice were used as a control. The following primers were used: *ywhag* common forward primer - 5'-TCATCAGCAGCATCGAGCAG-3'; *ywhag* WT reverse primer - 5'-ATGGCGTCGTCGAAGGC-3' and *ywhag* KO reverse primer - 5'-AGGGGTCTCTTTGTCAGGGT-3'. The PCR protocol was 95°C (10 min), then 35 cycles of 95°C (30 s), 58°C (30 s) 72°C (30 s), and 72°C (5 min). PCR products were examined using 1% agarose gel electrophoresis in TAE buffer.

### Western blotting

The whole brain tissues obtained were lysed using RIPA buffer containing a protease inhibitor cocktail (Roche) and processed for western blotting using anti-14-3-3 $\gamma$  antibody (sc-398423, 1:1000, Santa Cruz Biotechnology) and mouse anti-actin (1:2000; Sigma-Aldrich). Signals were detected using enhanced chemiluminescence (GE Healthcare, Chicago, IL, USA) following probing with the appropriate horseradish peroxidase-conjugated secondary antibodies (1:3000, Jackson ImmunoResearch). Each experiment was performed with samples from three independent groups.

### Behavioral tests

Animals were acclimatized to the behavior test room for a week before testing. Behavioral assays were commenced when the mice were aged 10 weeks. One cohort of mice were used for all behavioral assays (n=8 per genotype). The order of behavioral tests progresses from less stressful one (e.g. open field test) to more stressful one (e.g. forced swim test) and there were two or three day's interval between assays.

### Open field test

The open field test (OFT) was performed as described to measure locomotor activity [31]. The open field apparatus consisted of

a square arena (40×40 cm) with 30 cm high walls that was illuminated using an electric bulb hanging 2.5 m above the floor. Open field behaviors of the mice were recorded and analyzed using the ANY-maze system (Stoelting, Wood Dale, IL). Animals were exposed to the open field for 10 minutes. Between subjects, the box was thoroughly cleaned with 70% ethanol and the ethanol was allowed to evaporate completely prior to testing mice.

#### ***Elevated plus maze test***

The elevated plus maze (EPM) test was performed as described [32]. The apparatus consisted of two open arms and two enclosed arms arranged in a plus-sign orientation. The arms were elevated 50 cm above the floor with each 5-cm wide arm projecting 30 cm from the center. At the start of the test, each subject was placed in the center of the EPM facing a closed arm. Mice explored the maze for 5 minutes and exploratory activities in both the open and closed arms were recorded and analyzed using the ANY-maze system (Stoelting, Wood Dale, IL). Between subjects, the maze was thoroughly cleaned with 70% ethanol and the ethanol was allowed to evaporate completely prior to testing mice.

#### ***Light and dark box test***

This test was performed as described [33]. The apparatus consisted of two (light and dark) chambers (34×24×24 cm) joined together. There was an aperture (8×8 cm) between the two chambers that the mice could use to move between chambers. The chambers were made of white and black opaque Plexiglas. The black chamber was covered with a black lid (the dark box), while the white chamber was covered with a transparent lid and illuminated using ambient room lighting to ~450 lux (the light box). During the test, a subject was placed in the center of the light box facing away from the aperture connecting the two chambers and allowed to freely explore both chambers for 5 minutes. Between animals, the box was cleaned with 70% ethanol and allowed to completely dry. All sessions were recorded and analyzed using the ANY-maze system (Stoelting, Wood Dale, IL).

#### ***Social interaction test***

Mice were tested in a Plexiglas cage divided into three chambers comprising two equal-sized end areas (31.5×25.5 cm each) and a smaller neutral section between them (10.5×25.5 cm). During the habituation phase, the end areas contained an empty "holding cell" (10.16 cm in diameter and 13.97 cm tall). Each mouse was placed in the center of the box and allowed to explore the entire box for 5 minutes. The subject was then returned to the cage while another adult male (C57BL/6 WT mice) was placed under the holding cell (on one randomly selected side) and the empty cell was placed on

the opposite side. During the test phase, the subjects were placed in the center and allowed to investigate the entire box for 5 minutes. The ANY-maze system recorded and scored the number of entrances into each side and the time spent investigating the novel mouse. Investigation was defined as the test mouse's nose touching the novel mouse through the bars or sniffing within 1 cm. The test arena was carefully cleaned with 70% ethanol between subjects and allowed to completely dry.

#### ***Rotarod test***

The rotarod test was performed to evaluate the basic mobility of animals in each group as described [31]. Mice were placed on the stationary cylinder of the rotarod apparatus and trained on the apparatus for at least four consecutive trials in which the rod was kept at a constant speed (4 rpm) and returned to their cages for 1 min between trials. Once the animals were able to stay on the rod rotating at 4 rpm for at least 60 s, they were subjected to the rotarod test. Mice were placed on the rod rotating at an accelerating speed from 4 to 40 rpm over 300 s. The time before animals fell off the rod was recorded with a maximum cut-off of 300 s. Mice were tested for eight consecutive trials with at least 5-min intervals. The data from the last four trials were averaged as the latency to fall. Each mouse was returned to its home cage and remained there for 5 min before the next trial. If the mouse remained on the rod in 5 minutes, latency to fall was recorded as 300 s. Between subjects, the rotarod apparatus was thoroughly cleaned with 70% ethanol and allowed to completely dry.

#### ***Acute stress (restraint stress)***

Mice were subjected to a schedule of restraint stress before each behavior test to induce behavioral and physiological phenotypes. Each mouse was restrained using a 50 ml conical tube with an open end, exposing the nose for breathing. Acute stress was applied for one hour and each mouse was returned to its home cage immediately after restraining stress.

#### ***Statistical analysis***

All statistical analyses were carried out using GraphPad Prism version 5.00 for Windows. Numerical data are presented as means±standard error of the mean (SEM). The error bars in graphs denote the SEM. The statistical significance of the data was assessed using unpaired or paired Student's *t*-tests, with the significance level denoted by asterisks (\**p*<0.05, \*\**p*<0.01, or \*\*\**p*<0.001).

## RESULTS

**Generation and validation of the 14-3-3 $\gamma$  KO mice**

The genomic organization of the mouse 14-3-3 $\gamma$  gene (*ywhag*) and KO strategy using the gene trap system are illustrated (Fig. 1A and Fig. 2A) [30]. The sequence analysis of mRNA from 14-3-3 $\gamma$  homozygote pups showed that the exon 1, the partial exon 2 and the inserted sequence from the gene-trap pU-21W vector were ex-

pressed (Fig. 1B). This genetic insertion of foreign sequence results in truncated N-terminal 14-3-3 $\gamma$  peptide (71 amino acids of 14-3-3 $\gamma$  and 13 amino acid long peptide of gene-trap vector). This N-terminal fragment covers three initial domains (A~C) of 14-3-3 proteins (Fig. 1C).

To verify the genetic deletion of *ywhag* in mice, we performed PCR-based genotyping of tail samples of pups born from 14-3-3 $\gamma$  Het breeding pairs at P0 (Fig. 2B). We also examined the expres-

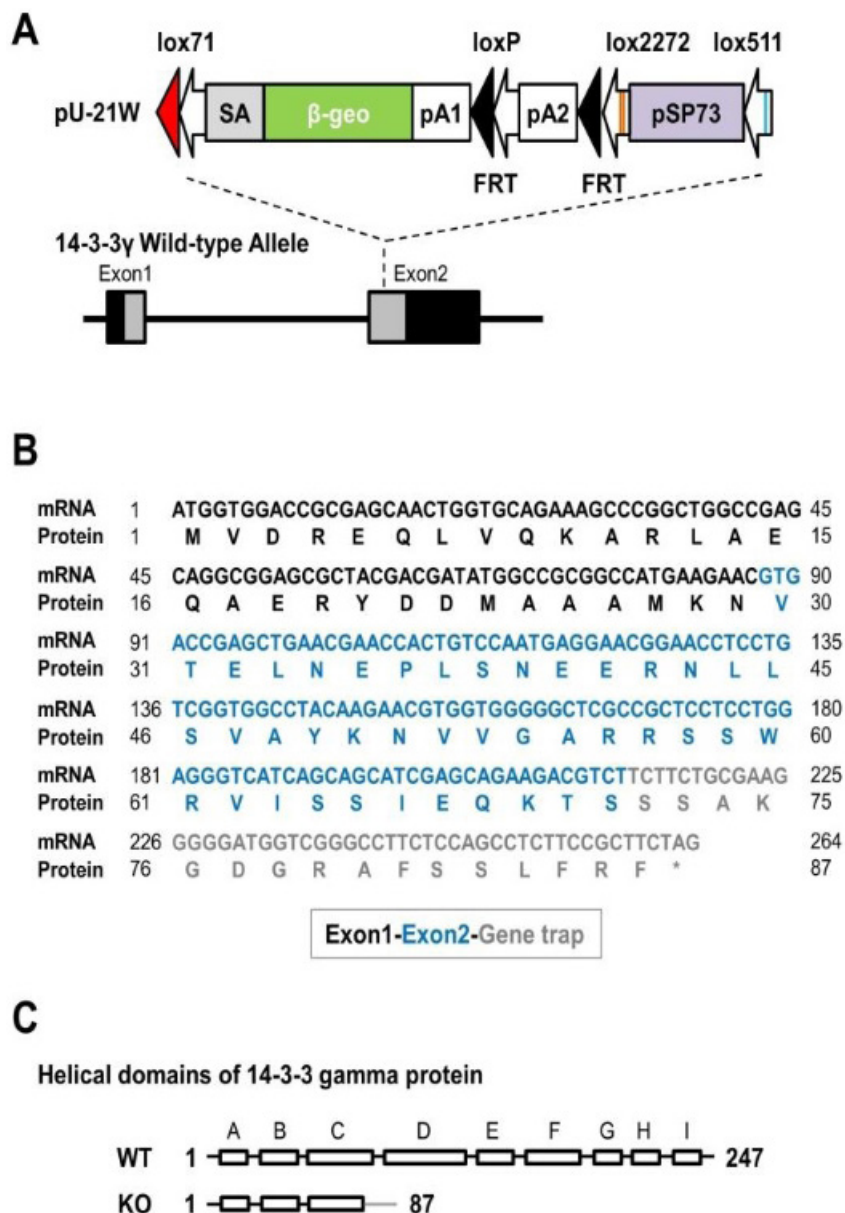


**Fig. 1.** Sequence analysis of targeted region of 14-3-3 $\gamma$  KO mice. (A) A genomic illustration of gene-trap strategy for 14-3-3 $\gamma$  KO mice. The organization of pU-21W trap-vector. EN2-intron, 1.2 kb of Mouse En2 intron 1; EN2-SA, splice acceptor of mouse En2 exon 2;  $\beta$ -geo,  $\beta$ -galactosidase; pA1, SV40 polyadenylation signal; pA2, mouse PGK gene polyadenylation signal; FRT, FLP recombinase target sequence. (B) The alignment of the mRNA sequences from RT-PCR of transgenic region and predicted protein sequence. (C) A map illustrates nine  $\alpha$ -helical domains of WT of 14-3-3 $\gamma$ , and mutant 14-3-3 $\gamma$  from these transgenic mice only has 3 N-terminal domains (A~C).

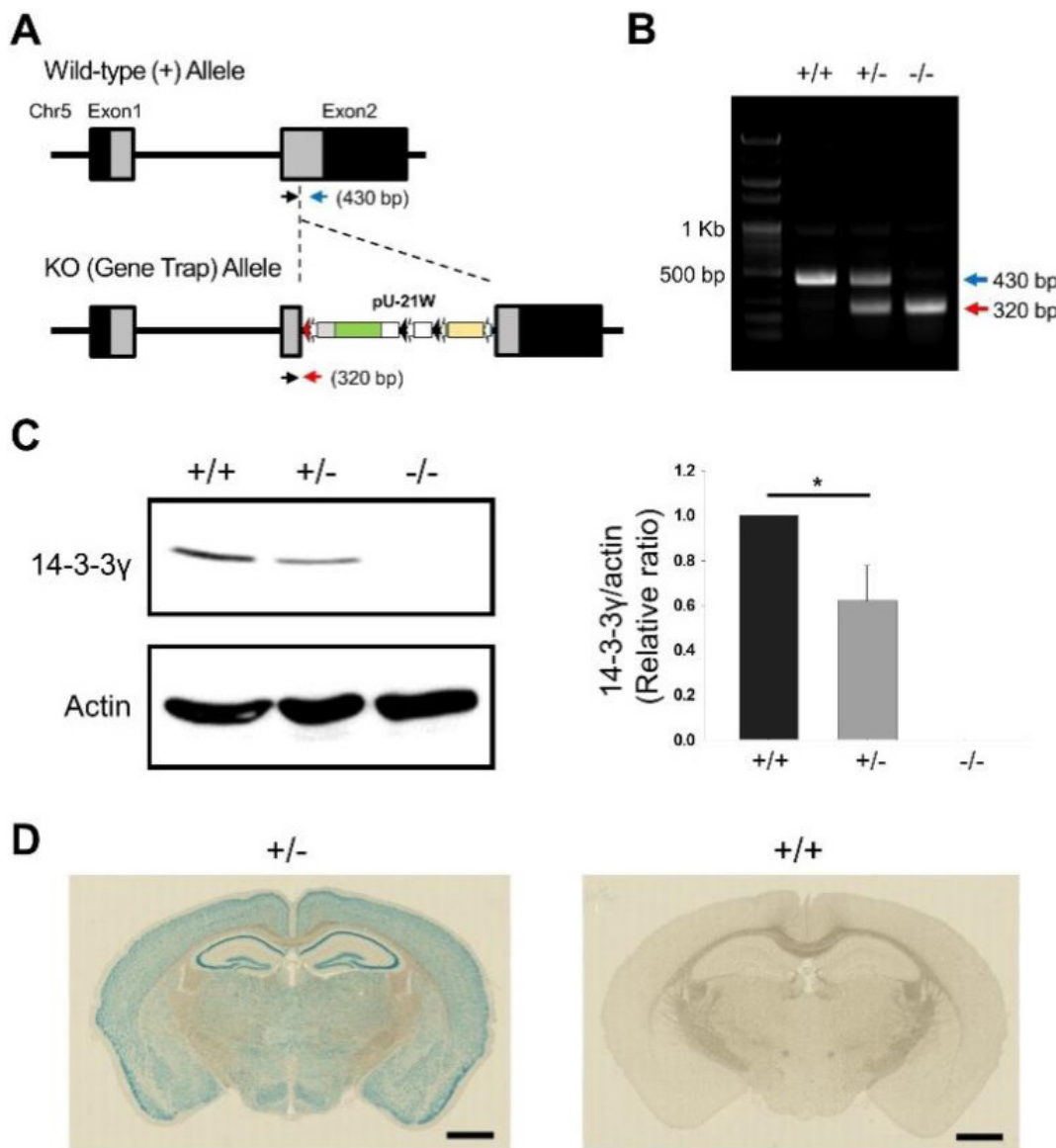


**Fig. 2.** Validation of 14-3-3 $\gamma$  KO mice. (A) A genomic illustration of 14-3-3 $\gamma$  KO mice. The trap vector, pU-21W, was inserted into the exon 2 of *ywhag*. Two PCR primers designed for exon 2 (black and blue arrows) and a primer for the trap vector (red arrow) were used for genotyping. (B) Genotyping result of genomic DNA prepared from 14-3-3 $\gamma$  WT, heterozygote, and homozygote KO mice. (C) (left) A representative western blot of brain homogenates prepared at P0 from 14-3-3 $\gamma$  WT, heterozygote, and homozygote KO mice using a specific 14-3-3 $\gamma$  antibody. (right) A bar graph showing the expression level of 14-3-3 $\gamma$  in the brain. (D)  $\beta$ -gal staining of 14-3-3 $\gamma$  Het and WT mice. Scale bar: 1 mm.

sion level of 14-3-3 $\gamma$  using a specific anti-14-3-3 $\gamma$  antibody with brain homogenates prepared from pups at P0 (Fig. 2C). It is noted that the 14-3-3 $\gamma$  signal from homozygote KO mice was absent, and the level of 14-3-3 $\gamma$  from heterozygote (Het) mice was significantly reduced compared to that in littermate control mice. These data indicate that *ywhag* gene was successfully disrupted in these 14-3-3 $\gamma$  KO mice. Beta-gal staining of adult Het mice showed the broad expression of 14-3-3 $\gamma$  in the brain (Fig. 2D). Since  $\beta$ -geo expression in 14-3-3 $\gamma$  Het mice is controlled by the endogenous promoter of the *ywhag* gene [30],  $\beta$ -geo expression in our 14-3-3 $\gamma$

Het mice represents the endogenous expression pattern of 14-3-3 $\gamma$ . The  $\beta$ -geo expression clearly showed in the pyramidal layer of the hippocampus, and its expression pattern is consistent with the mRNA expression pattern of 14-3-3 $\gamma$  in the Allen brain atlas database (<http://mouse.brain-map.org/experiment/show?id=1124>).

Interestingly, at weaning (P21), we found that there were no surviving homozygote KO mice among the 242 mice born from 15 breeding pairs (36 litters of pups) (Fig. 3A). This is clearly distinct from the other two homozygote KO mice of 14-3-3 isoform genes (*ywhae* and *ywhaz*) that survive long enough for behavioral ex-

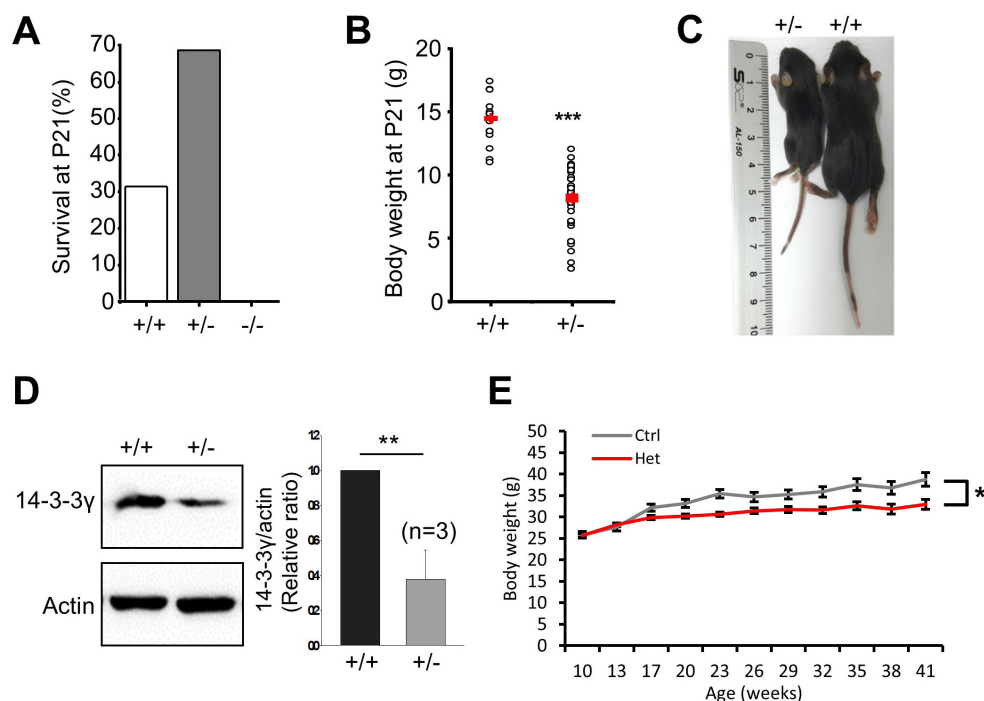


**Fig. 3.** 14-3-3 $\gamma$  Het mice are smaller and lighter. (A) A summary bar graph showing the survival rate of pups at P21 born from 14-3-3 $\gamma$  Het breeding pairs. (B) A summary bar graph showing the body weights of pups born from 14-3-3 $\gamma$  Het breeding pairs at P21. (C) A photographic image of 14-3-3 $\gamma$  WT and Het mice at P21. (D) (left) A representative western blot of brain homogenates prepared from 14-3-3 $\gamma$  WT and Het adult mice using a specific 14-3-3 $\gamma$  antibody. (right) A summary bar graph showing the expression level of 14-3-3 $\gamma$ . (E) A summary graph showing the body weights of 14-3-3 $\gamma$  WT and Het mice used in behavioral experiments.

periments [10, 11]. In addition, we also noticed that the body size and weight of 14-3-3 $\gamma$  Het mice was significantly less than those of littermate controls (Fig. 3B and 3C). Based on these data, we concluded that 14-3-3 $\gamma$  is critically important for the maturation and survival of mice in contrast to a previous report [29]. We also examined the expression level of 14-3-3 $\gamma$  using brain homogenates prepared from adult 14-3-3 $\gamma$  WT and Het mice and found that the reduced expression of 14-3-3 $\gamma$  in Het mice was maintained (Fig. 3D). For behavioral experiments, we selected Het mice as similar as possible in size and body weight to WT littermate controls to see whether differences in behavioral phenotypes were directly related to the genetic disruption of 14-3-3 $\gamma$ . We also measured the body weights of the two genotypes throughout adulthood until we finished the behavioral experiments (Fig. 3E).

#### 14-3-3 $\gamma$ Het mice are hyperactive

Since 14-3-3 $\gamma$  is abundantly expressed in the brain, to investigate its role in the expression of behavioral characteristics, we performed an OFT to assess basal locomotor activity. Intriguingly, 14-3-3 $\gamma$  Het mice traveled significantly more distance in the center zone than WT mice (Fig. 4A), which may be due to hyperactivity and not related to less anxiety, because the total distance traveled

and mean speed of 14-3-3 $\gamma$  Het mice were significantly longer and faster than those in WT mice, respectively (Fig. 4B and 4C). In addition, the Het mice also showed significant longer margin distance compared to WT mice (data not shown). Because there was no significant difference between WT and Het mice in the rotarod test, any change in muscle strength or coordination of Het mice was not related (Fig. 4D).

#### 14-3-3 $\gamma$ Het mice show depressive-like behavior

Since the OFT suggested that the reduced level of 14-3-3 $\gamma$  in Het mice results in hyperactive behavior, to determine whether the 14-3-3 $\gamma$  haploinsufficiency may affect mood-related behaviors, we conducted the forced swim test (FST) and three-chamber social interaction test (3CT). Interestingly, Het mice displayed significantly longer immobile time in the FST than WT mice (Fig. 5A), which suggests that their depressive-like phenotype was induced by 14-3-3 $\gamma$  haploinsufficiency, while there was no deficit in the social interaction of Het mice in the 3CT (Fig. 5B).

#### 14-3-3 $\gamma$ Het mice show more sensitive responses to acute stress

Hyperactive and depressive symptoms are common in patients

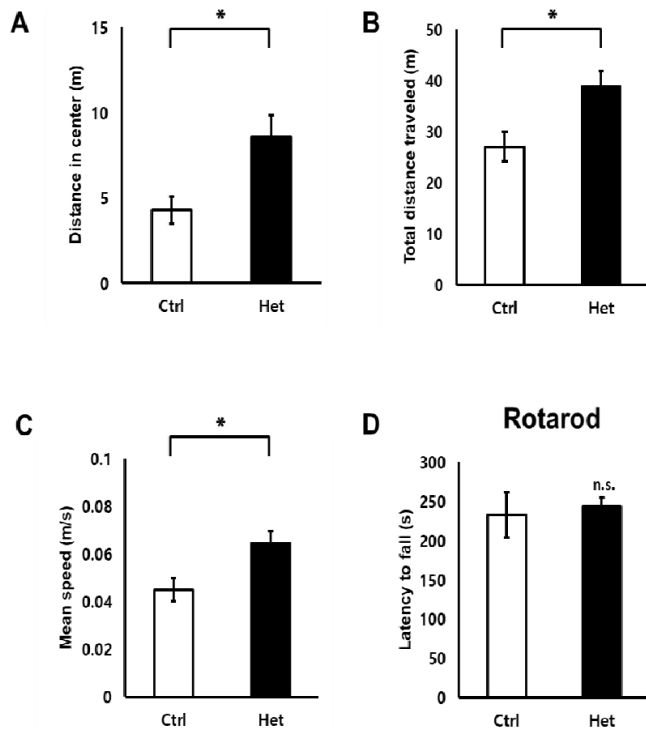
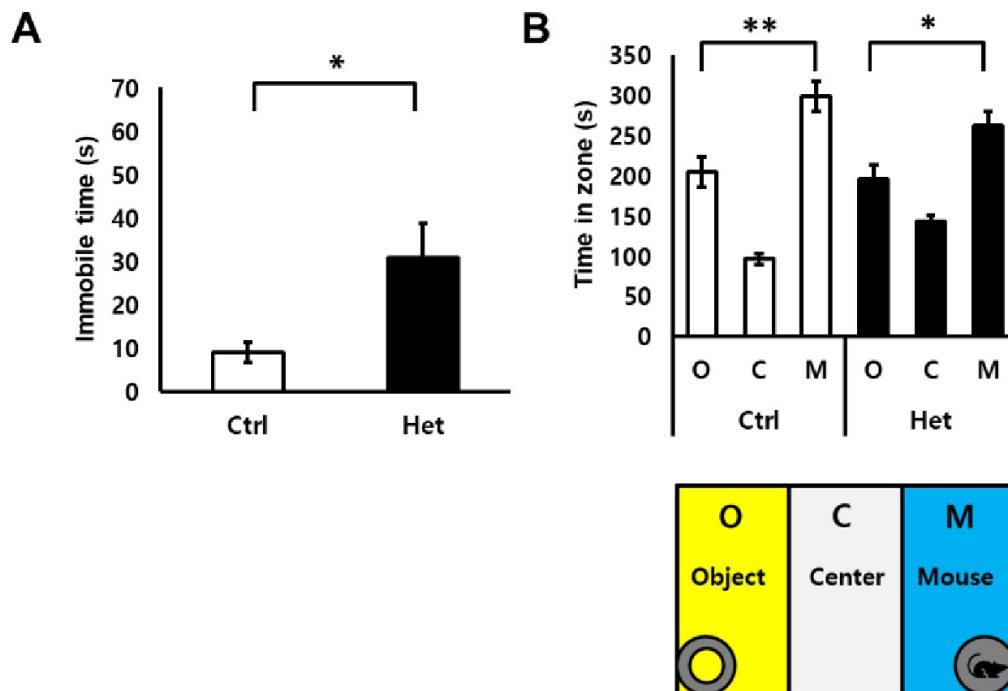


**Fig. 4.** Hyperactivity in 14-3-3γ Het mice is not due to altered baseline motor activity. (A) Locomotor activity in an OFT, quantified as distance traveled in the center zone. (B) Locomotor activity in an OFT, quantified as total distance traveled. (C) Average traveling speed in an OFT. (D) Latency to fall in accelerated rotarod test (n=8 mice/genotype, \*p<0.05, n.s. not statistically significant).

with several neuropsychiatric diseases. Since these patients often have a deficit in the appropriate response to acute stress [34], we subjected Het mice to restraint stress and performed several behavioral tests including the OFT, light and dark box (LDB) test, and EPM test. In the OFT, the hyperactivity of Het mice was significantly decreased, as seen in the total distance traveled and mean speed (Fig. 6A and 6B), while WT littermate control mice did not show any significant change. In the LDB test, total distance traveled in the light zone and number of transitions were significantly increased in Het mice in response to acute stress (Fig. 6C and 6D). Similarly, Het mice showed significantly increased time spent in open ends and total distance traveled in open arms in response to acute stress in the EPM test (Fig. 6E and 6F).

**DISCUSSION**

14-3-3γ proteins play diverse roles in many different cellular processes [1, 3, 23, 24]. In addition to the role as an adaptor protein facilitating protein-protein interactions in diverse cellular signaling processes, 14-3-3γ has been shown to be involved in transporting ion channels, transporters, and transmembrane receptors to the plasma membrane such as BK channels, TRPM4, ANO1, and BEST-1 in excitable and non-excitable cells [26-28, 36]. Furthermore, 14-3-3γ has been implicated in several neurological and psychiatric diseases such as spinocerebellar ataxia type 1, Parkinson’s disease, and tuberous sclerosis [15-17]. Especially,



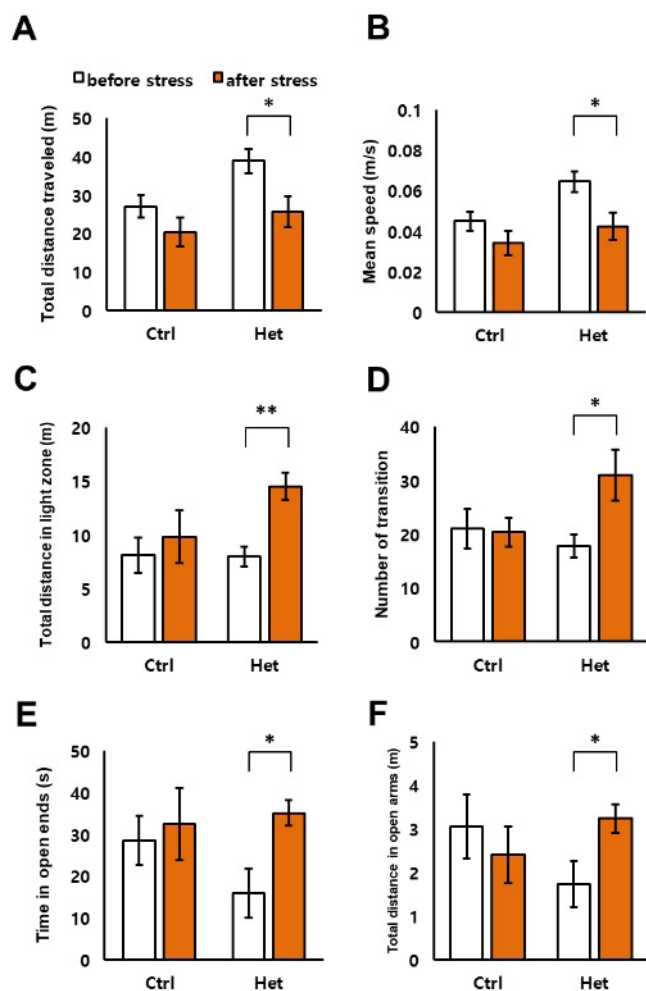


**Fig. 6.** The sensitive response to acute stress in 14-3-3 $\gamma$  Het mice. Stress response in an OFT, quantified as total distance traveled (A), and mean speed (B). Stress response in a LDB test, quantified as a total distance traveled in the light zone (C) and number of transitions (D). Stress response in an EPM test, quantified as time in the open ends (E) and total distance traveled in the open arms (F). (n=8 mice/genotype, \*p<0.05, \*\*p<0.01).

recent studies showed that *de novo* mutations of the *ywhag* gene or duplication/deletion of chromosomal regions including *ywhag* cause neurodevelopmental disorders in human [18-21, 37, 38].

Unlike the potential significance of 14-3-3 $\gamma$  in brain development from these studies, a previous study showed that 14-3-3 $\gamma$  null mice display no apparent behavioral abnormalities [29]. These 14-3-3 $\gamma$  KO mice were generated by the genomic replacement of exon 2 with neomycin resistance cassette to delete exon 2 of 14-3-3 $\gamma$  [29]. Authors of this study suggested that other endogenous 14-3-3 isoforms may compensate for the loss of 14-3-3 $\gamma$ . In contrast, we found that 14-3-3 $\gamma$  homozygous KO mice were prenatally lethal, and heterozygous mice showed developmental delay relative to littermate wild-type mice (Fig. 2 and 3). In our mice, the *ywhag* gene was disrupted by inserting a gene-trap vector in the middle

of exon 2. Our 14-3-3 $\gamma$  KO mice express truncated 84-amino acid fragment containing the partial exon 2 and foreign gene from gene trap vector (Fig. 1). Since the N-terminal part of 14-3-3 $\gamma$  has been shown to be important in dimerization of 14-3-3 $\gamma$ , it is possible that this extra sequence may interfere in the function of 14-3-3 $\gamma$  in its expressing cells [39].

In behavioral experiments, we found that 14-3-3 $\gamma$  Het mice display hyperactive locomotor activity, and more sensitive responses to acute stress than WT mice. Hyperactive locomotor activity, observed in the OFT, was not due to any alteration in muscle strength or endurance since there was no significant difference in latency to fall in the rotarod test between WT and Het mice. 14-3-3 $\gamma$  Het mice showed significantly increased depressive-like behavior in the FST relative to WT mice. After exposure to acute stress, we observed that the hyperactivity feature of Het mice was significantly reduced in the OFT. On the other hand, Het mice showed increased travel distance in the light zone and number of transitions in the LDB test, as well as increased distance and time spent in the open arms in the EPM test. Based on these stress-response behaviors, reduced level of 14-3-3 $\gamma$  in Het mice may increase the sensitivity to exogenous stimuli relative to WT. Although this study clearly showed the significant relevance of 14-3-3 $\gamma$  in mouse behaviors, the correlation between cell-type specific expressions of 14-3-3 $\gamma$  in the brain and its related behavioral phenotypes need to be examined in detail.

Hyperactivity and hypersensitivity are frequently observed as comorbid symptoms in many neuropsychiatric diseases, such as attention deficit hyperactivity disorder (ADHD). Hyperactivity has multiple manifestations, including continuous movement, being distracted, and impulsive behaviors. ADHD patients with hypersensitivity are highly agitated when faced with various challenges including sensory stimuli and psychological stress. This condition makes individuals overactive and inattentive from unknown causes, which often prohibits individuals from living normal lives [40]. Interestingly, the behavioral phenotypes of our 14-3-3 $\gamma$  Het mice display two characteristics of ADHD (Fig. 4~6). Recently, WBS, a 14-3-3 $\gamma$ -related neurodevelopmental disease, has been shown to be strongly associated with ADHD with hyperactivity and hypersensitivity [41, 42]. Since 14-3-3 $\gamma$  Het mice displayed neurodevelopmental delay, hypersensitivity and hyperactivity, we believe that our 14-3-3 $\gamma$  Het mice can be a good mouse model for ADHD and WBS.

There are features of 14-3-3 $\gamma$  distinct from the other 14-3-3 proteins although functions of 14-3-3 isoforms seem to be redundant and their expression patterns in organisms are vastly overlapping [35, 43, 44]. For example, the elevated level of 14-3-3 $\gamma$  in the brain has been considered a potential biomarker in Creutzfeldt-Jakob



disease [44]. In an animal model of multiple sclerosis and ischemia, 14-3-3 $\gamma$  has been reported to play significant roles [35, 43]. In addition, reduced expression of 14-3-3 $\gamma$  in zebrafish caused deficits in brain development and decreased brain size [38] and altered expression of 14-3-3 $\gamma$  in mice delayed neuronal migration in the cerebral cortex [23, 24]. Therefore, our 14-3-3 $\gamma$  Het mice may also be valuable to study the pathophysiological mechanisms of these diseases.

#### AUTHOR CONTRIBUTIONS

D.E.K., C-H.C., K.M.S., O.K., and E.M.H. performed the experiments. D.E.K., C-H.C., K.M.S., E.M.H., H-W.K., and J-Y.P. interpreted the data. C-H.C., D.K., E.M.H., H-W.K., and J-Y.P. designed the study and wrote the paper.

#### ACKNOWLEDGEMENTS

This work was supported by the National Research Foundation (NRF) of Korea (NRF-2016M3C7A1904149, NRF-2017M3A9C6027009 and NRF-2017M3A9C4092979 to JYP, NRF-2017R1D1A1B03032212 to C-HC, NRF-2016R1D-1A1B03933283 to HWK).

#### REFERENCES

1. Aghazadeh Y, Papadopoulos V (2016) The role of the 14-3-3 protein family in health, disease, and drug development. *Drug Discov Today* 21:278-287.
2. Cornell B, Toyono-Oka K (2017) 14-3-3 proteins in brain development: neurogenesis, neuronal migration and neuromorphogenesis. *Front Mol Neurosci* 10:318.
3. Kaplan A, Morquette B, Kroner A, Leong S, Madwar C, Sanz R, Banerjee SL, Antel J, Bisson N, David S, Fournier AE (2017) Small-molecule stabilization of 14-3-3 protein-protein interactions stimulates axon regeneration. *Neuron* 93:1082-1093.e5.
4. Mackintosh C (2004) Dynamic interactions between 14-3-3 proteins and phosphoproteins regulate diverse cellular processes. *Biochem J* 381:329-342.
5. Zhang J, Zhou Y (2018) 14-3-3 proteins in glutamatergic synapses. *Neural Plast* 2018:8407609.
6. Kent CB, Shimada T, Ferraro GB, Ritter B, Yam PT, McPherson PS, Charron F, Kennedy TE, Fournier AE (2010) 14-3-3 proteins regulate protein kinase A activity to modulate growth cone turning responses. *J Neurosci* 30:14059-14067.
7. Yam PT, Kent CB, Morin S, Farmer WT, Alchini R, Lepelletier L, Colman DR, Tessier-Lavigne M, Fournier AE, Charron F (2012) 14-3-3 proteins regulate a cell-intrinsic switch from sonic hedgehog-mediated commissural axon attraction to repulsion after midline crossing. *Neuron* 76:735-749.
8. Qiao H, Foote M, Graham K, Wu Y, Zhou Y (2014) 14-3-3 proteins are required for hippocampal long-term potentiation and associative learning and memory. *J Neurosci* 34:4801-4808.
9. Foote M, Qiao H, Graham K, Wu Y, Zhou Y (2015) Inhibition of 14-3-3 proteins leads to schizophrenia-related behavioral phenotypes and synaptic defects in mice. *Biol Psychiatry* 78:386-395.
10. Cheah PS, Ramshaw HS, Thomas PQ, Toyono-Oka K, Xu X, Martin S, Coyle P, Guthridge MA, Stomski F, van den Buuse M, Wynshaw-Boris A, Lopez AE, Schwarz QP (2012) Neurodevelopmental and neuropsychiatric behaviour defects arise from 14-3-3 $\zeta$  deficiency. *Mol Psychiatry* 17:451-466.
11. Wachi T, Cornell B, Toyono-Oka K (2017) Complete ablation of the 14-3-3 epsilon protein results in multiple defects in neuropsychiatric behaviors. *Behav Brain Res* 319:31-36.
12. Dougherty MK, Morrison DK (2004) Unlocking the code of 14-3-3. *J Cell Sci* 117:1875-1884.
13. Lai XJ, Ye SQ, Zheng L, Li L, Liu QR, Yu SB, Pang Y, Jin S, Li Q, Yu AC, Chen XQ (2014) Selective 14-3-3 $\gamma$  induction quenches p- $\beta$ -catenin Ser37/Bax-enhanced cell death in cerebral cortical neurons during ischemia. *Cell Death Dis* 5:e1184.
14. Peoc'h K, Schröder HC, Laplanche J, Ramljak S, Müller WE (2001) Determination of 14-3-3 protein levels in cerebrospinal fluid from Creutzfeldt-Jakob patients by a highly sensitive capture assay. *Neurosci Lett* 301:167-170.
15. Rosner M, Hanneder M, Siegel N, Valli A, Hengstschläger M (2008) The tuberous sclerosis gene products hamartin and tuberin are multifunctional proteins with a wide spectrum of interacting partners. *Mutat Res* 658:234-246.
16. Umahara T, Uchihara T, Yagishita S, Nakamura A, Tsuchiya K, Iwamoto T (2007) Intracellular immunolocalization of 14-3-3 protein isoforms in brains with spinocerebellar ataxia type 1. *Neurosci Lett* 414:130-135.
17. Shimada T, Fournier AE, Yamagata K (2013) Neuroprotective function of 14-3-3 proteins in neurodegeneration. *BioMed Res Int* 2013:564534.
18. Coe BP, Stessman HA, Sulovari A, Geisheker MR, Bakken TE, Lake AM, Dougherty JD, Lein ES, Hormozdiari F, Bernier RA, Eichler EE (2019) Neurodevelopmental disease genes implicated by *de novo* mutation and copy number variation morbidity. *Nat Genet* 51:106-116.
19. Fusco C, Micale L, Augello B, Teresa Pellico M, Menghini D,

- Alfieri P, Cristina Digilio M, Mandriani B, Carella M, Palumbo O, Vicari S, Merla G (2014) Smaller and larger deletions of the Williams Beuren syndrome region implicate genes involved in mild facial phenotype, epilepsy and autistic traits. *Eur J Hum Genet* 22:64-70.
20. Ramocki MB, Bartnik M, Szafranski P, Kołodziejska KE, Xia Z, Bravo J, Miller GS, Rodriguez DL, Williams CA, Bader PI, Szczepanik E, Mazurczak T, Antczak-Marach D, Coldwell JG, Akman CI, McAlmon K, Cohen MP, McGrath J, Roeder E, Mueller J, Kang SH, Bacino CA, Patel A, Bocian E, Shaw CA, Cheung SW, Mazurczak T, Stankiewicz P (2010) Recurrent distal 7q11.23 deletion including HIP1 and YWHAG identified in patients with intellectual disabilities, epilepsy, and neurobehavioral problems. *Am J Hum Genet* 87:857-865.
21. Nicita F, Garone G, Spalice A, Savasta S, Striano P, Pantaleoni C, Sparta MV, Kluger G, Capovilla G, Pruna D, Freri E, D'Arrigo S, Verrotti A (2016) Epilepsy is a possible feature in Williams-Beuren syndrome patients harboring typical deletions of the 7q11.23 critical region. *Am J Med Genet A* 170A:148-155.
22. Watanabe M, Isobe T, Ichimura T, Kuwano R, Takahashi Y, Kondo H (1993) Molecular cloning of rat cDNAs for beta and gamma subtypes of 14-3-3 protein and developmental changes in expression of their mRNAs in the nervous system. *Brain Res Mol Brain Res* 17:135-146.
23. Cornell B, Wachi T, Zhukarev V, Toyo-Oka K (2016) Overexpression of the 14-3-3gamma protein in embryonic mice results in neuronal migration delay in the developing cerebral cortex. *Neurosci Lett* 628:40-46.
24. Wachi T, Cornell B, Marshall C, Zhukarev V, Baas PW, Toyooka K (2016) Ablation of the 14-3-3gamma protein results in neuronal migration delay and morphological defects in the developing cerebral cortex. *Dev Neurobiol* 76:600-614.
25. Chen XQ, Chen JG, Zhang Y, Hsiao WW, Yu AC (2003) 14-3-3gamma is upregulated by *in vitro* ischemia and binds to protein kinase Raf in primary cultures of astrocytes. *Glia* 42:315-324.
26. Cho CH, Kim E, Lee YS, Yarishkin O, Yoo JC, Park JY, Hong SG, Hwang EM (2014) Depletion of 14-3-3 $\gamma$  reduces the surface expression of Transient Receptor Potential Melastatin 4b (TRPM4b) channels and attenuates TRPM4b-mediated glutamate-induced neuronal cell death. *Mol Brain* 7:52.
27. Lee YS, Lee JK, Bae Y, Lee BS, Kim E, Cho CH, Ryoo K, Yoo J, Kim CH, Yi GS, Lee SG, Lee CJ, Kang SS, Hwang EM, Park JY (2016) Suppression of 14-3-3 $\gamma$ -mediated surface expression of ANO1 inhibits cancer progression of glioblastoma cells. *Sci Rep* 6:26413.
28. Oh SJ, Woo J, Lee YS, Cho M, Kim E, Cho NC, Park JY, Pae AN, Justin Lee C, Hwang EM (2017) Direct interaction with 14-3-3 $\gamma$  promotes surface expression of Best1 channel in astrocyte. *Mol Brain* 10:51.
29. Steinacker P, Schwarz P, Reim K, Brechlin P, Jahn O, Kratzin H, Aitken A, Wiltfang J, Aguzzi A, Bahn E, Baxter HC, Brose N, Otto M (2005) Unchanged survival rates of 14-3-3gamma knockout mice after inoculation with pathological prion protein. *Mol Cell Biol* 25:1339-1346.
30. Kurogi S, Sekimoto T, Funamoto T, Ota T, Nakamura S, Nagai T, Nakahara M, Yoshinobu K, Araki K, Araki M, Chosa E (2017) Development of an efficient screening system to identify novel bone metabolism-related genes using the exchangeable gene trap mutagenesis mouse models. *Sci Rep* 7:40692.
31. Choi WS, Kim HW, Tronche F, Palmiter RD, Storm DR, Xia Z (2017) Conditional deletion of Ndufs4 in dopaminergic neurons promotes Parkinson's disease-like non-motor symptoms without loss of dopamine neurons. *Sci Rep* 7:44989.
32. Zou J, Wang W, Pan YW, Abel GM, Storm DR, Xia Z (2015) Conditional inhibition of adult neurogenesis by inducible and targeted deletion of ERK5 MAP kinase is not associated with anxiety/depression-like behaviors. *eNeuro* 2:ENEURO.0014-14.2015.
33. Zou J, Storm DR, Xia Z (2013) Conditional deletion of ERK5 MAP kinase in the nervous system impairs pheromone information processing and pheromone-evoked behaviors. *PLoS One* 8:e76901.
34. Zimmerman EC, Bellaire M, Ewing SG, Grace AA (2013) Abnormal stress responsivity in a rodent developmental disruption model of schizophrenia. *Neuropsychopharmacology* 38:2131-2139.
35. Lee DH, Steinacker P, Seubert S, Turnescu T, Melms A, Manzel A, Otto M, Linker RA (2015) Role of glial 14-3-3 gamma protein in autoimmune demyelination. *J Neuroinflammation* 12:187.
36. Sokolowski B, Orchard S, Harvey M, Sridhar S, Sakai Y (2011) Conserved BK channel-protein interactions reveal signals relevant to cell death and survival. *PLoS One* 6:e28532.
37. Guella I, McKenzie MB, Evans DM, Buerki SE, Toyota EB, Van Allen MI, Suri M, Elmslie F, Simon ME, van Gassen KL, Héron D, Keren B, Nava C, Connolly MB, Demos M, Farrer MJ, Adam S, Boelman C, Bolbocean C, Candido T, Eydoux P, Horvath G, Huh L, Nelson TN, Sinclair G, van Karnebeek C, Vercauteren S; Epilepsy Genomics Study; Deciphering Developmental Disorders Study (2017) *De novo* mutations in YWHAG cause early-onset epilepsy. *Am J Hum Genet* 101:300-310.
38. Komoike Y, Fujii K, Nishimura A, Hiraki Y, Hayashidani M,

- Shimajima K, Nishizawa T, Higashi K, Yasukawa K, Saitsu H, Miyake N, Mizuguchi T, Matsumoto N, Osawa M, Kohno Y, Higashinakagawa T, Yamamoto T (2010) Zebrafish gene knockdowns imply roles for human YWHAG in infantile spasms and cardiomegaly. *Genesis* 48:233-243.
39. Aghazadeh Y, Ye X, Blonder J, Papadopoulos V (2014) Protein modifications regulate the role of 14-3-3 $\gamma$  adaptor protein in cAMP-induced steroidogenesis in MA-10 Leydig cells. *J Biol Chem* 289:26542-26553.
40. Randazzo WT, Dockray S, Susman EJ (2008) The stress response in adolescents with inattentive type ADHD symptoms. *Child Psychiatry Hum Dev* 39:27-38.
41. Rhodes SM, Riby DM, Matthews K, Coghill DR (2011) Attention-deficit/hyperactivity disorder and Williams syndrome: shared behavioral and neuropsychological profiles. *J Clin Exp Neuropsychol* 33:147-156.
42. Uljarević M, Labuschagne I, Bobin R, Atkinson A, Hocking DR (2018) Brief report: the impact of sensory hypersensitivity and intolerance of uncertainty on anxiety in Williams syndrome. *J Autism Dev Disord* 48:3958-3964.
43. Platholi J, Heerdt PM, Lim Tung HY, Hemmings HC Jr (2008) Activation of brain protein phosphatase-1(I) following cardiac arrest and resuscitation involving an interaction with 14-3-3 $\gamma$ . *J Neurochem* 105:2029-2038.
44. Humpel C, Benke T (2017) Cerebrospinal fluid levels of 14-3-3 $\gamma$ : what does it tell us about sporadic Creutzfeldt-Jakob disease? *Pharmacology* 100:243-245.